Fine Structure and Dynamics of the Solar Atmosphere
Proceedings IAU Symposium No. 327, 2016
S. Vargas Domínguez, A.G. Kosovichev, P. Antolin & L. Harra, eds.

doi:10.1017/S1743921317000126

Granular cells in the presence of magnetic field

J. Jurčák[1], B. Lemmerer[2] and M. van Noort[3]

[1]Astronomical Institute ASCR, Fričova 298, 251 65 Ondřejov, Czech Republic
email: jurcak@asu.cas.cz

[2]Institute of Physics, IGAM, University of Graz, Universitätsplatz 5, 8010 Graz, Austria
email: birgit.lemmerer@uni.graz.at

[3]Max-Planck-Institut für Sonnensystemforschung, Justus-von-Liebig-Weg 3, 37077 Göttingen, Germany
email: vannoort@mps.mpg.de

Abstract. We present a statistical study of the dependencies of the shapes and sizes of the photospheric convective cells on the magnetic field properties. This analysis is based on a 2.5 hour long SST observations of active region NOAA 11768. We have blue continuum images taken with a cadence of 5.6 sec that are used for segmentation of individual granules and 270 maps of spectropolarimetric CRISP data allowing us to determine the properties of the magnetic field along with the line-of-sight velocities. The sizes and shapes of the granular cells are dependent on the the magnetic field strength, where the granules tend to be smaller in regions with stronger magnetic field. In the presence of highly inclined magnetic fields, the eccentricity of granules is high and we do not observe symmetric granules in these regions. The mean up-flow velocities in granules as well as the granules intensities decrease with increasing magnetic field strength.

Keywords. Sun: granulation, Sun: photosphere, techniques: polarimetric

1. Introduction

The majority of the solar surface is covered by granulation, convective cells that are heating the photosphere. The properties of granules in the quiet Sun regions are well described. Numerous studies show that there are no characteristic sizes of granular cells, but the mean size amounts to values between 1" and 2" (e.g., Wohl & Nordlund 1985; Roudier & Muller 1986; Hirzberger *et al.* 1997; Danilovic *et al.* 2008). Abramenko *et al.* (2012) found a distinct population of small convective cells with a dominant spatial scale below 600 km. These small granules were also found in high resolution solar radiation hydrodynamics simulations by Lemmerer *et al.* (2014).

Granulation is also present in active regions. There are a number of case studies showing the properties of convective cells in the presence of magnetic field. In the extreme case of sunspot umbra, the magneto-convection results into the umbral dots (see e.g., Schussler & Vogler 2006; Ortiz *et al.* 2010). In the sunspot penumbra, where the field is weaker and more horizontal, the magneto-convective cells are highly elongated and form penumbral filaments (see e.g., Rempel 2011; Tiwari *et al.* 2013). Broad sunspot light bridges show a granular pattern where the properties of convective cells are comparable to the quiet Sun granules (Lagg *et al.* 2014), but they are smaller and have longer lifetimes (Hirzberger *et al.* 2002). Very elongated granules are typically observed in flux emergence regions (Schlichenmaier *et al.* 2010; Centeno *et al.* 2016) and granules in plage regions are typically smaller and exhibit lower velocities than field-free granulation (Narayan & Scharmer 2006).

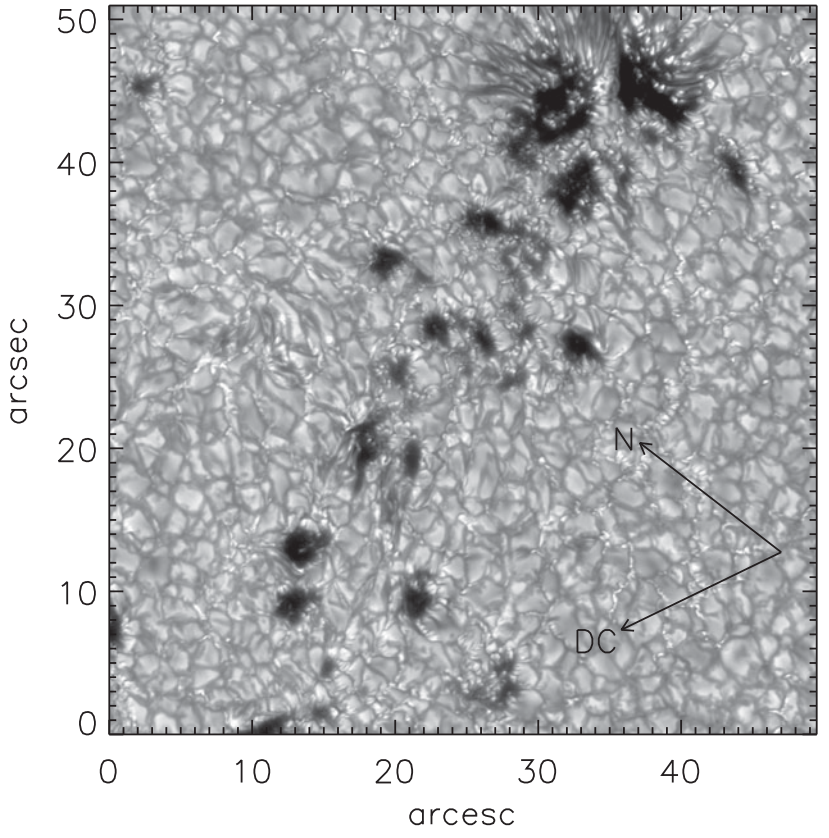

Figure 1. Blue continuum image of the observed region of NOAA 11768 on June 13, 2013 at 10:30 UT. The arrows point to the solar north and solar disc centre.

To our knowledge, the influence of the magnetic field on the properties of the solar granulation has not yet been approached statistically. We apply this approach to the SST data introduced in Sect. 2. The first results are described in Sect. 3 and discussed in Sect. 4.

2. Observations and data analysis

The evolution of active region NOAA 11768 was observed on June 13, 2013 using the Swedish Solar Telescope (Scharmer *et al.* 2003). In Fig. 1, we show the blue continuum image of the analysed field of view (FOV). It contains the leading polarity sunspot in active region NOAA 11768 and part of the following polarity. This active region appeared on the solar disc on June 11, 2013 and at the time of observations, the intensive flux emergence was still observed.

Blue continuum images reconstructed with the MOMFBD technique (van Noort *et al.* 2005) have a cadence of 5.6 s, spatial sampling of 0.034“, and were recorded between 8:21 UT and 10:50 UT. The CRISP observations (Scharmer *et al.* 2008) of the Stokes profiles of the Fe I 525 nm line were taken with a cadence of 31 s, spatial sampling of 0.055”, and were recorded between 8:36 UT and 10:54 UT.

The imaging and CRISP data were co-aligned. The blue continuum images are used for the segmentation of granules using the algorithm described in Lemmerer *et al.* (2014). The spectropolarimetric CRISP data are used to derive the magnetic field strength,

https://doi.org/10.1017/S1743921317000126 Published online by Cambridge University Press

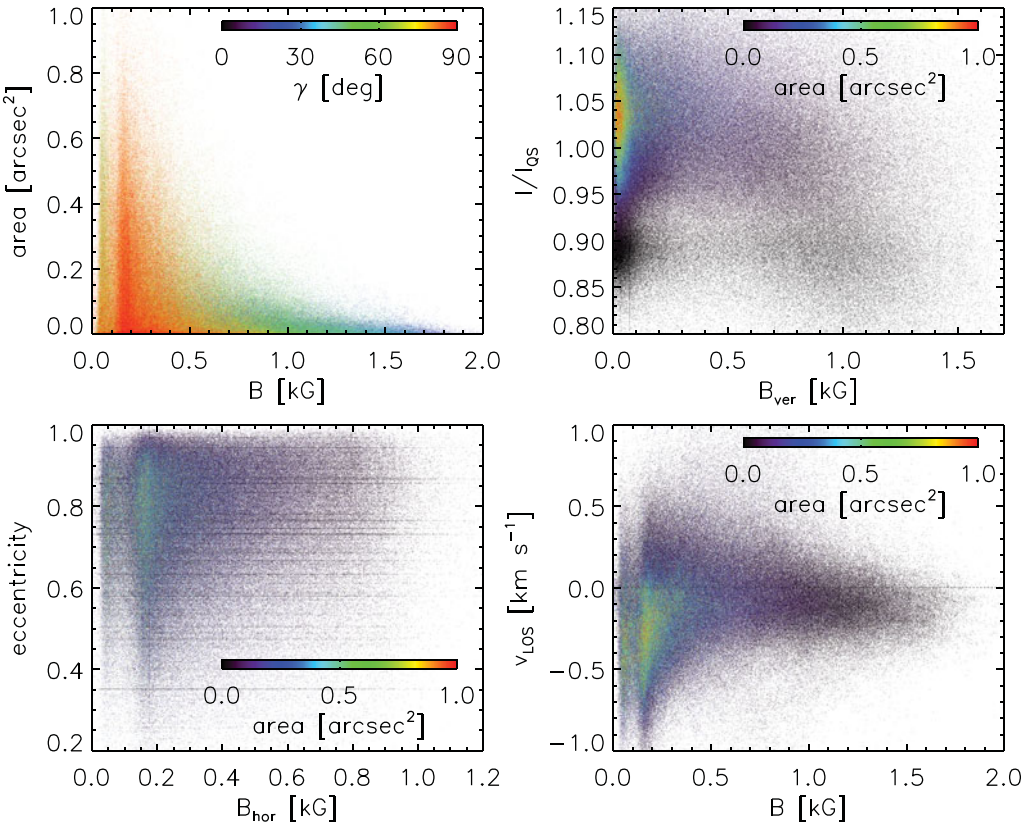

Figure 2. Maps of magnetic field strength (upper left), magnetic field inclination (upper right), segmented intensity image (lower left), and LOS velocity (lower right) co-spatial and co-temporal with Fig. 1. Regions with $B < 200$ G are masked out in γ map.

inclination, and azimuth along with the LOS velocity. We used the Milne-Eddington inversion code VFISV (Borrero *et al.* 2011). The 180° ambiguity was solved using the code AMBIG (Leka *et al.* 2009) and the magnetic field inclination and azimuth were transformed to the local reference frame using the AZAM routines (Lites *et al.* 1995).

3. Results

In Fig. 2, we show an example of the resulting maps of physical properties in the studied region along with the results of the segmentation algorithm. In the observed FOV, we have all kinds of granulation, from convection in non-magnetised regions (upper-left and lower-right regions of the FOV), through flux emergence regions (around x and y coordinates [15", 30"] and [25", 15"]), granulation in the close vicinity of pores, granular light bridges, penumbral filaments and umbral dots.

Using the segmentation results, we computed for every identified granule in every CRISP scan its area and eccentricity (fitting an ellipse to the granule), mean intensity, mean velocity, mean magnetic field strength and inclination. Currently, we do not take into account the temporal evolution of granules and do not track them from one scan to another.

In Fig. 3, we show scatter plots illustrating the influence of the magnetic field on the properties of convective cells. The upper left plot shows that the maximum size of

https://doi.org/10.1017/S1743921317000126 Published online by Cambridge University Press

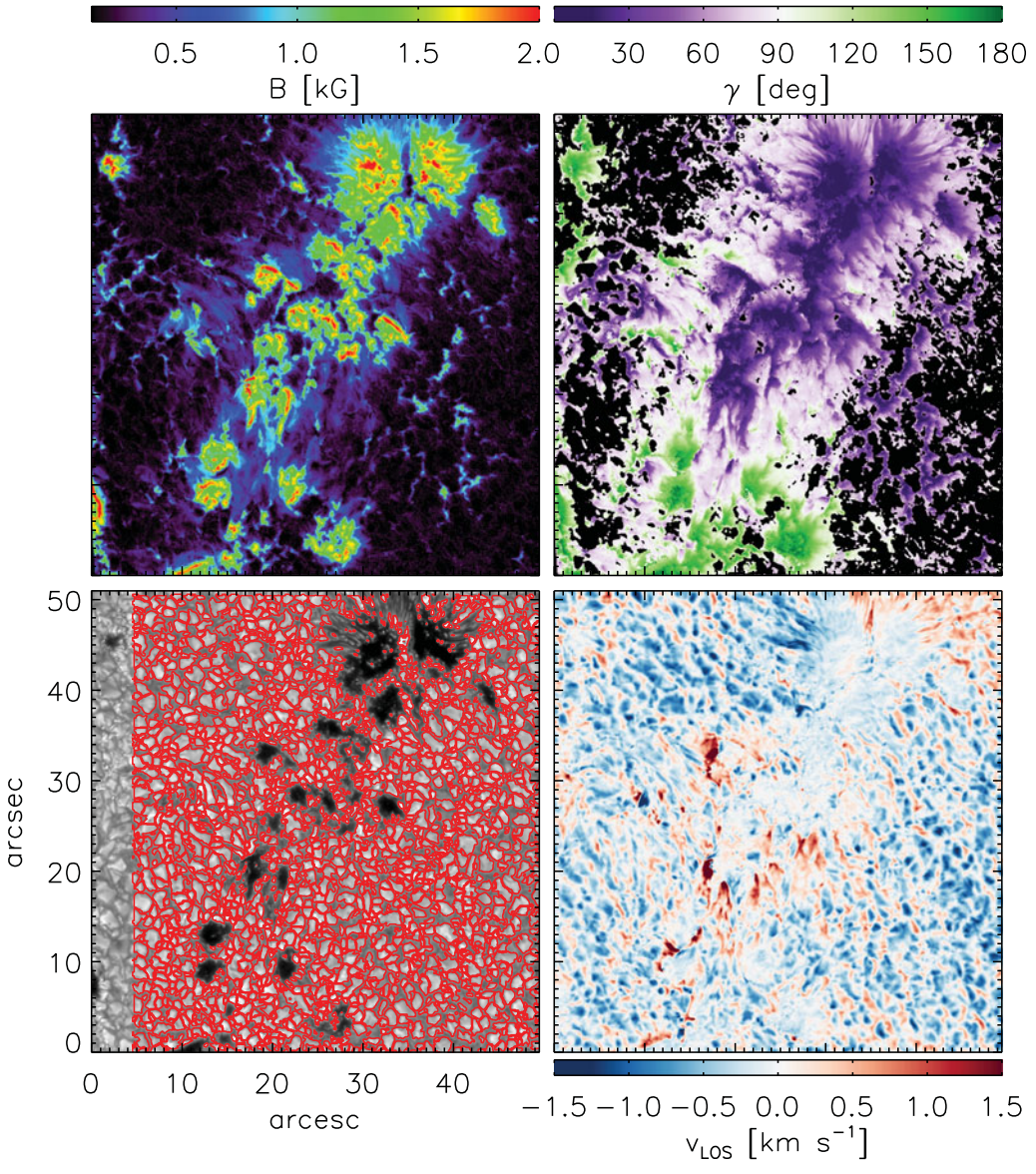

Figure 3. Scatter plots showing the dependences of the granules size on the magnetic field strength (upper left), the granules intensities on the $B_{\rm ver}$ (upper right), the granules eccentricities on the $B_{\rm hor}$ (lower left), and the LOS velocities in the granules on the magnetic field strength (lower right).

convective cells is significantly dependent on the magnetic field strength. The largest granules are observed in non-magnetic regions, whereas the smallest ones correspond to the umbral dots in the sunspot. The colour-coded magnetic field inclination indicates that the strongest fields in the FOV are close to vertical. Please note that due to the simplistic inversion scheme, we do obtain some magnetic field strength in all regions of the FOV and that the weak fields are close to horizontal.

The upper right plot in Fig. 3 shows the dependence of the mean granular intensity on the vertical component of the magnetic field. The higher the $B_{\rm ver}$ is, the lower is the

https://doi.org/10.1017/S1743921317000126 Published online by Cambridge University Press

mean intensity of the granule. In this scatter plot, we also see the population of small non-magnetised granules that have lower intensities than regular granules (Abramenko *et al.* 2012; Lemmerer *et al.* 2014).

The lower left plot in Fig. 3 shows that the eccentricity of observed granules depends on the horizontal component of the magnetic field. In regions with weak $B_{\rm hor}$, we observe granules of all eccentricities. The higher $B_{\rm hor}$ is, the less frequent are the more symmetric granules. As the granules are difficult to fit by ellipses, we need to investigate other approaches to access the influence of the $B_{\rm hor}$ on the elongation of the convective cells.

The lower right plot in Fig. 3 shows the influence of the magnetic field strength on the mean LOS velocity in the convective cells. As expected, the higher B is, the lower is $v_{\rm LOS}$. There is a distinct population of mainly small granules with positive $v_{\rm LOS}$, i.e., showing on average a plasma down-flow. Such down-flows in small granules were observed by Yu *et al.* (2011) and they are found also in simulations (Gadun *et al.* 2000; Lemmerer *et al.* 2014).

4. Discussion and conclusions

We investigated statistically the properties of convective cells in the presence of a magnetic field. The analysed FOV of the SST observations covered all kinds of granulation, from convection in the quiet Sun to the sunspot magneto-convection. The first results confirm the previous case studies of convection in the presence of a magnetic field.

The convective cells are getting smaller with increasing field strength. The intensity of granules is decreasing with increasing vertical component of the magnetic field. However, there is a population of small non-magnetised granules that have comparable intensities to those in regions with strong $B_{\rm ver}$. In the presence of strong horizontal fields, we more likely observe asymmetric granules compared to non-magnetised regions. This is in particular related to the flux emergence regions, where highly elongated granules connect the opposite polarity patches. The mean up-flow velocity in the granules decreases with increasing magnetic field strength. There is also a distinct population of predominantly smaller granules exhibiting down-flows that need to be investigated in detail.

The next crucial step is to take into account the temporal evolution of individual granules, i.e., apply a tracking algorithm to the segmented granules. This step will allow us not only to investigate the dependence of the lifetime of convective cells on the magnetic field strength, but also elaborate the currently presented results by taking into account the evolution of the magnetic field properties and LOS velocities during the lifetime of the individual convective cells. We also need to filter the segmentation results for falsely identified granules, e.g., magnetic bright points and penumbral bright grains.

Acknowledgements

J. J. acknowledges the financial support by the Grant Agency of the Czech Republic through the grant 14-04338S and the project RVO:67985815. J. J. and B. L. acknowledge the financial support from ÖAD and MŠMT in frame of the bilateral project 7AMB16AT010. B. L. acknowledges the financial support from the Austrian Science Fund (FWF): P27765. The Swedish 1-m Solar Telescope is operated on the island of La Palma by the Institute for Solar Physics of the Royal Swedish Academy of Sciences in the Spanish Observatorio del Roque de los Muchachos of the Instituto de Astrofísica de Canarias.

References

Abramenko, V. I., Yurchyshyn, V. B., Goode, P. R., Kitiashvili, I. N., & Kosovichev, A. G. 2012, *ApJ*, 756, L27

Borrero, J. M., Tomczyk, S., Kubo, M., Socas-Navarro, H., Schou, J., Couvidat, S., & Bogart, R. 2011, *Solar Phys.*, 273, 267

Centeno, R., Blanco Rodriguez, J., Del Toro Iniesta, J. C., Solanki, S. K., Barthol, P., Gandorfer, A., Gizon, L., Hirzberger, J., Riethmuller, T. L.. van Noort, M., Orozco Suarez, D., Schmidt, W., Martinez Pillet, V., & Knolker, M. 2016, *arXiv*, 2016arXiv161003531C

Danilovic, S., Gandorfer, A., Lagg, A., Schüssler, M., Solanki, S. K., Vögler, A., Katsukawa, Y., & Tsuneta, S. 2008, *A&A*, 484, 17

Gadun, A. S., Hanslmeier, A., Pikalov, K. N., Ploner, S. R. O., Puschmann, K. G., & Solanki, S. K. 2000 *A&AS*, 146, 267

Hirzberger, J., Vázquez, M., Bonet, J. A., Hanslmeier, A., & Sobotka, M. 1997 *ApJ*, 480, 406

Hirzberger, J., Bonet, J. A., Sobotka, M., Vázquez, M., & Hanslmeier, A. 2002 *A&A*, 383, 275

Leka, K. D., Barnes, G., & Crouch, A. 2009 *ASPC*, 415, 365

Lemmerer, B., Utz, D., Hanslmeier, A., Veronig, A., Thonhofer, S., Grimm-Strele, H., & Kariyappa, R. 2014 *A&A*, 563, 107

Lemmerer, B., Hanslmeier, A., Muthsam, H., & Piantschitsch 2016 *arXiv*, 2016arXiv161106786L

Lites, B. W., Low, B. C., Martinez Pillet, V., Seagraves, P., Skumanich, A., Frank, Z. A., Shine, R. A., & Tsuneta, S. 1995 *ApJ*, 446, 877

Narayan, G, & Scharmer, G. B. 2010 *A&A*, 524, 3

Ortiz, A., Bellot Rubio, L. R., & Rouppe van der Voort, L. 2010 *ApJ*, 713, 1282

Rempel, M. 2011 *ApJ*, 740, 15

Roudier, T., & Muller, R. 1986 *Solar Phys.*, 107, 11

Scharmer, G. B., Bjelksjo, K., Korhonen, T. K., Lindberg, B., & Petterson, B. 2003 *SPIE*, 4853, 341

Scharmer, G. B., Narayan, G., Hillberg, T., de la Cruz Rodriguez, J., Löfdahl, M. G., Kiselman, D., Sütterlin, P., van Noort, M., & Lagg, A. 2008 *ApJ*, 689, 69

Schlichenmaier, R., Bello González, N., Rezaei, R., & Waldmann, T. A. 2010 *AN*, 331, 563

Schüssler, M., & Vögler, A. 2006 *ApJ*, 641, 73

Tiwari, S. K., van Noort, M., Lagg, A., & Solanki, S. K. 2013 *A&A*, 557, 25

van Noort, M., Rouppe van der Voort, L., & Löfdahl, M. G. 2005 *Solar Phys.*, 228, 191

Woehl, H., & Nordlund, A. 1985 *Solar Phys.*, 97, 213

Yu, D., Xie, Z., Hu, Q., Yang, S., Zhangm, J., & Wang, J. 2011 *ApJ*, 743, 58